Determination of the long-range order parameter from the tetragonality ratio of $L1_0$ alloys

Nadi Braidy, Yann Le Bouar,* and Mathieu Fèvre
Laboratoire d'Étude des Microstructures, CNRS–ONERA, 29 Avenue de la Division Leclerc, BP 72, 92322 Châtillon Cedex, France

Christian Ricolleau
Matériaux et Phénomènes Quantiques, CNRS–Université Paris 7–Denis Diderot, 4 rue Elsa Morante, Bâtiment Condorcet, Case Courrier 7021, 75205 Paris Cedex, France

(Received 17 July 2009; revised manuscript received 11 November 2009; published 1 February 2010)

A method to calculate the long-range order parameter, (LROP, η) of a $L1_0$ phase from its tetragonality ratio (c/a) is proposed. The equation builds on the original derivation of [Roberts, Acta Metall. **2**, 597 (1954)], deduced from the analysis of nearest neighbors but includes the effect of the anisotropy of the lattice thermal expansion and is extended to include off-stoichiometric alloys. In order to explore the range of validity of the proposed formula, Monte Carlo simulations were performed using a Lennard-Jones-type potential which mimics the $L1_0$-solid solution transformation. It is shown that the new formula corrects a systematic bias introduced when the anisotropy of the thermal-expansion coefficients is ignored. The gain in accuracy with respect to Roberts' formula is appreciable, especially for alloys exhibiting both a strong anisotropy of the lattice expansion coefficients and a low tetragonality ratio. When approaching the transition temperature and for alloys with increasing deviation from stoichiometry, the precision of the proposed formula degrades and the physical origin of this behavior is discussed. The equation is offered as a simple, bias-free, and precise method to evaluate the order parameter of a bulk alloy from the tetragonality ratio deduced from typical *in situ* x-ray diffraction measurements.

DOI: 10.1103/PhysRevB.81.054202 PACS number(s): 64.60.Cn, 75.40.Cx, 02.70.Uu, 64.60.De

I. INTRODUCTION

A number of binary *A*-*B* alloys crystallize in the $L1_0$ phase at low temperature. The interest of these alloys lies in their properties owing to their particular crystalline structure. Technologically relevant examples of such alloys include systems in which *A* is a magnetic 3*d* element and *B* is a 4*d* or 5*d* element (e.g., CoPt, FePt, and NiPt). These alloys exhibit a very large magnetocrystalline anisotropy and make them excellent candidates for future ultrahigh-density recording media.[1,2]

Ordered, $L1_0$ structures typically have a tetragonal unit cell that will be herein considered, for convenience, as a face-centered-cubic (fcc) lattice slightly compressed in the [001] direction, whose lattice parameters are denoted *a* and *c* (see Fig. 1). The $L1_0$ structure can be described as an alternate stacking of *A*-rich and *B*-rich (002) planes. The chemistry of the $A_{1/2+\delta}B_{1/2-\delta}$ $L1_0$ alloy is characterized by two quantities: the deviation from stoichiometry δ and the long-range order parameter (LROP) η, that is hereafter defined as the difference between the composition of the *A*-rich and *B*-rich (002) planes.

Several relevant physical properties are directly related to the LROP. For example, it was experimentally[3] and theoretically[4] shown that for FePt alloys, the magnetocrystalline anisotropy changes by a factor of 2 when the order parameter increases from 0.9 to 1.0. Therefore, the knowledge of the LROP is highly desirable and constitutes an asset for materials design, especially in the fields of high density and magneto-optic recording.

The LROP is usually measured from x-ray powder-diffraction experiments. Indeed, the diffraction pattern of a $L1_0$ structure exhibits superstructure reflections due to the chemical ordering in the unit cell. The square of the order parameter can then be deduced from the integrated intensities under the fundamental (assigned to the fcc lattice) and superstructures reflexions. However, a precise measurement of the LROP requires for each peak the precise determination of the Lorentz polarization factor, the absorption correction, the extinction factor, and the Debye-temperature factor. In addition, if texture is present, the deduction of LROP will be biased if measured using the integrated intensity of x-ray Bragg peaks.

Because the lattice parameters *a* and *c* are easily and accurately measured from x-ray diffraction, Roberts proposed, in a seminal work on stoichiometric Cu-Au alloys, to simply deduce the value of the order parameter from the tetragonality ratio, $\kappa(=c/a)$. Using a simplified model based on the occurrence of *A*-*A*, *B*-*B*, and *A*-*B* first nearest-neighbor atomic pairs, Roberts proposed the following equation:[5]

$$\eta_R^2 = \frac{\mathcal{B}}{4}(1-\kappa), \tag{1}$$

where the numerical value of the $\mathcal{B}/4$ prefactor is obtained using an experimental value of κ taken at a low temperature T_0, at which the alloy is considered completely ordered $[\eta(T_0)=1$ for a stoichiometric alloy].

Equation (1), initially derived for bulk Cu-Au alloys, has been extensively applied to determine the LROP in various types of $L1_0$ bulk homogenized alloys: CoPt, FePd,[6] FePt,[7] NiMn,[8] and PtMn,[9] and later to thin films,[8,10–12] multilayers,[1,7,13] ion-irradiated thin films and nanoparticles.[14,15] Although the original formula was derived for a stoichiometric alloy, it was used[6,10,16] and somewhat adapted[17] to alloys having a deviation from stoichiometry. The accuracy of Roberts' equation has been addressed by

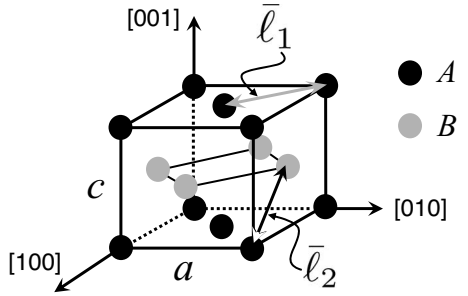

FIG. 1. Schematic of the $L1_0$ fully ordered structure, where A and B atoms occupy the site of a face-centered tetragonal cell with a and c lattice parameters.

several reports by comparing the LROP obtained from Eq. (1) to the one obtained from the integrated intensities of the fundamental and the superstructure reflexions: in Ref. 17, an excellent agreement between both methods is observed whereas in Ref. 1, significant differences in the calculation of the LROP (up to 26%) were reported. Moreover, Seki *et al.* raised serious concerns regarding the applicability of Roberts' formula to epitaxially grown thin films.[10]

We can also question the validity of Roberts' formula in bulk alloys from experimental data. Indeed, given that the LROP systematically decreases with temperature, it is obvious from Roberts' formula that the c/a ratio should increase monotonically with temperature. However, it is clear from Fig. 2 that the c/a ratios measured in NiPt, CoPt, and FePd $L1_0$ alloys decrease over a low-temperature range. Consequently, the use of Roberts' formula in these alloys (with a prefactor $\mathcal{B}$ deduced from c/a ratio at 300 K) yields a LROP above unity at higher temperatures, which is nonphysical.

Given the widespread use of this formula in the analysis and the interpretation of diffraction-related experiments realized on $L1_0$ alloys, it seems essential to revisit its underlying assumptions and rectify the formula to widen its range of validity. In this paper, we first derive an improved version of Roberts' formula, valid for stoichiometric as well as nonstoichiometric $L1_0$ alloys, where the influence of the lattices thermal-expansion coefficients is taken into account. Then, we numerically test the accuracy of the new formula and discuss the validity of the underlying assumptions. The numerical tests are performed using Monte Carlo (MC) simulations of $L1_0$ alloys with a position-dependent interatomic potential. We finally describe precisely the usage of the equation and discuss its applicability to different materials microstructures.

II. THEORY

The aim of the model proposed by Roberts was to relate the LROP of a $L1_0$ structure to its c/a ratio. The idea was to start from a $L1_0$ structure with a given LROP, η, and to consider the first nearest-neighbor atom pairs of type A-A, B-B, and A-B. Each kind of pair has a reference length, referred to as ℓ_{AA}, ℓ_{BB}, or ℓ_{AB}, which represents the optimal bond length of the pair in the structure. The first hypothesis of Roberts' approach was to consider the mean bond length of the first nearest-neighbor pairs in a given direction equal

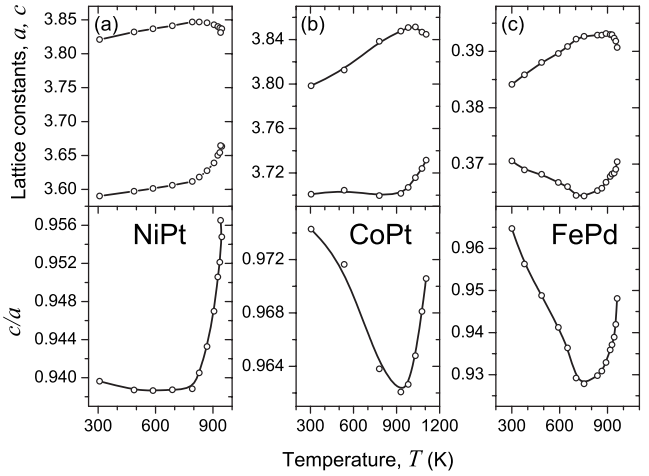

FIG. 2. Experimental lattice parameters (top) and tetragonality ratio (bottom) as a function of temperature for (a) NiPt (Ref. 18), (b) CoPt (Ref. 18), and (c) FePd (Ref. 19). Data were graphically extracted from the cited references.

to the average of the reference bond lengths in the same direction, weighted by the relative proportion of each type of atom in the pair. Using this approach, we can define the average lengths, $\bar{\ell}_1$ and $\bar{\ell}_2$, as the separation of nearest-neighbor pairs, respectively, within and between (002) planes (see Fig. 1). Finally, the value of the c/a ratio is geometrically computed using the ratio of $\bar{\ell}_2$ to $\bar{\ell}_1$.

The reason for estimating the bond length from the relative occurrence of each possible atomic pair was not explicitly justified in Roberts' paper. It is interesting to realize that this approach can be derived from the minimization of a simplified spring-based energetic model. The model can be understood by describing the crystalline structure as a set of atoms in which the nearest neighbors are connected by springs of equal stiffness. The bond length corresponds to the spring length and would be defined by either ℓ_{AA}, ℓ_{BB}, or ℓ_{AB}, depending on the type of the atomic connecting pair. Minimizing the elastic energy of this model with respect to a homogeneous quadratic deformation of the crystal also leads to the model proposed by Roberts. This energetic derivation demonstrates that Roberts' approach is only justified within the framework of a simplified energetic model (spring model, with the same spring constants for all type of pairs, homogeneous deformation).

An additional assumption was to consider that ℓ_{AA} and ℓ_{BB} are proportional to the lattice constants of their respective components (pure A or B metal). Therefore, due to thermal expansion, the reference lengths are necessarily temperature dependent. This point, which was omitted in Roberts' paper, has important consequences, which will be discussed below.

The second hypothesis of Roberts' approach was to consider that the probability of two atoms being first nearest-neighbor atomic pair is simply the product of the concentrations of each atomic site (single-site mean-field approximation). The validity of this assumption, related to the importance of short-range order in the $L1_0$ structure, will be addressed in the discussion.

Following Roberts' original derivation, we now rederive the relation between the LROP and the c/a ratio to include the effect of thermal expansion, and we extend the validity of the formula to nonstoichiometric $L1_0$ alloys. Only the important steps of the derivation are given in this section with some details in Appendix.

Consider an ordered $A_{1/2+\delta}B_{1/2-\delta}$, $L1_0$ structure which admits a deviation from stoichiometry δ. Let C^α and C^β, the concentration of A atoms in two successive (002) planes, with α and β planes being rich in A and B atoms, respectively. The concentration C^α and C^β are related to δ and the LROP η through

$$C^\alpha = \delta + \frac{1+\eta}{2}, \tag{2a}$$

$$C^\beta = \delta + \frac{1-\eta}{2}. \tag{2b}$$

Following Roberts, the average first nearest neighbors distance within (002) planes, $\bar{\ell}_1$, and those between two (002) planes, $\bar{\ell}_2$(see Fig. 1), can be written as

$$\bar{\ell}_1 = \frac{1}{2}\sum_{ij}(P_{ij}^\alpha \ell_{ij} + P_{ij}^\beta \ell_{ij}), \tag{3a}$$

$$\bar{\ell}_2 = \sum_{ij} P_{ij}^{\alpha\beta}\ell_{ij}, \tag{3b}$$

where P_{ij}^α, P_{ij}^β, and $P_{ij}^{\alpha\beta}$ are the probabilities of finding a first nearest-neighbor atomic pair of type ij (ij=AA, BB, or AB) in the A-rich (002) planes, B-rich (002) planes, and between A-rich and B-rich planes, respectively.

Within the single-site mean-field approximation, the pair probabilities are related to the atomic site concentrations given in Eq. (2) (cf. Appendix.) and the ratio, $K=\bar{\ell}_2/\bar{\ell}_1$, can be expressed as

$$K(\delta) = \frac{\bar{\ell}_2}{\bar{\ell}_1} = \frac{\ell(\delta) - \frac{\eta^2}{4}\mathcal{L}^-}{\ell(\delta) + \frac{\eta^2}{4}\mathcal{L}^-}, \tag{4}$$

where

$$\ell(\delta) = \frac{1}{4}\mathcal{L}^+ + (\ell_{AA} + \ell_{BB})\delta + \mathcal{L}^-\delta^2 \tag{5a}$$

with

$$\mathcal{L}^+ = \ell_{AA} + \ell_{BB} + 2\ell_{AB}, \tag{5b}$$

$$\mathcal{L}^- = \ell_{AA} + \ell_{BB} - 2\ell_{AB}. \tag{5c}$$

From the geometry of the $L1_0$ cell (Fig. 1), $K(\delta)$ is related to $\kappa=c/a$,

$$K(\delta) = \sqrt{\frac{1+\kappa(\delta)^2}{2}}. \tag{6}$$

By isolating the LROP in Eq. (4), we obtain a relation between κ and the order parameter (through K),

$$\eta^2 = \frac{1}{\theta}\frac{1-K}{1+K} \tag{7}$$

in which

$$\theta(\delta) = \frac{\mathcal{L}^-}{4\ell(\delta)}. \tag{8}$$

The fact that κ in $L1_0$ structures is close to unity, entitles us to the following Taylor expansion around 1:

$$\frac{1-K}{1+K} = \frac{1}{4}(1-\kappa) - \frac{3}{64}(1-\kappa)^3 - \frac{1}{32}(1-\kappa)^4 + \cdots. \tag{9}$$

Given that the second-order term vanishes, we can expect the first-order term of the Taylor expansion to be highly accurate for realistic values of κ; typically, the relative error is below 5×10^{-4} for κ values ranging between 0.9 and 1. The error introduced by neglecting the higher-order terms is insignificant with respect to other sources, as it will be discussed below. Thus, Eq. (7) reduces to

$$\eta^2 = \frac{1}{4\theta(\delta,T)}(1-\kappa). \tag{10}$$

As in the formula proposed by Roberts, a linear relationship is found between the square of the LROP and the c/a ratio. However, in Eq. (10) the prefactor is not a constant and depends both on temperature and on the deviation from stoichiometry.

The dependence of the prefactor $\theta(\delta,T)$ on δ appears explicitly in Eq. (8). Its temperature dependence takes origin from the thermal expansion associated to the reference lengths. Assuming a linear thermal expansion, the reference lengths can be written as

$$\ell_{ij} = \ell_{ij}^0(1+\alpha_{ij}\Delta T) \tag{11}$$

with $\Delta T=T-T_0$, where T_0 is the low-temperature reference, α_{ij} is the corresponding linear-expansion coefficient of the ℓ_{ij} bond, and ℓ_{ij}^0 is the bond length at T_0.

The order of magnitude of α_{ij} is similar to that of a lattice-parameter thermal-expansion coefficient, i.e., about 10^{-5} K^{-1}. Therefore, the temperature variations in the reference lengths are very small. It is then possible to expand Eq. (8) to the first order in ΔT (see Appendix), which leads to a linear dependence of θ with temperature,

$$\theta(\delta) \approx \theta_0(\delta)[1+\alpha_\theta(\delta)\Delta T]. \tag{12}$$

Equation (12) would only be useful if the coefficients $\theta_0(\delta)$ and $\alpha_\theta(\delta)$ can be related to quantities that can be measured experimentally. This can be achieved using the low-temperature behavior of the LROP and the lattice parameters a and c.

When the temperature is low enough, roughly when T is lower than $T^*/2$, where T^* is the $L1_0$/fcc transition temperature, the LROP can be considered constant and equal to its maximum value $\eta_\delta=1-2|\delta|$ (this point will be further discussed in Sec. V B). In this temperature range, the evolution

of the lattice parameters a and c is only due to thermal expansion, and a linear evolution of the lattice parameters with temperature can be assumed,

$$a(\delta) = a_0(\delta)[1 + \alpha_a(\delta)(T - T_0)], \tag{13a}$$

$$c(\delta) = c_0(\delta)[1 + \alpha_c(\delta)(T - T_0)]. \tag{13b}$$

$a_0(\delta)$ and $c_0(\delta)$ are the lattice parameters at low temperature ($T=T_0$). $\alpha_a(\delta)$ and $\alpha_c(\delta)$ are the linear-expansion coefficients of the corresponding lattice constant. These quantities can be deduced from the measurements of the lattice parameters of a sample with a deviation from stoichiometry, δ, provided that the annealing time is long enough to ensure that equilibrium is reached. Following these considerations, the θ parameter of Eq. (10) can be evaluated as

$$\theta(\delta) = \frac{1}{4(1-2|\delta|)^2}\left\{1 - \frac{c_0(\delta)}{a_0(\delta)}\frac{[1 + \alpha_c(\delta)\Delta T]}{[1 + \alpha_a(\delta)\Delta T]}\right\}. \tag{14}$$

The parameters of Eq. (12) become, following a first-order expansion around ΔT,

$$\theta_0(\delta) = \frac{1 - \kappa_0(\delta)}{4(1-2|\delta|)^2},$$

$$\alpha_\theta(\delta) = \frac{\kappa_0(\delta)}{1 - \kappa_0(\delta)}[\alpha_a(\delta) - \alpha_c(\delta)], \tag{15}$$

where $\kappa_0(\delta) = c_0(\delta)/a_0(\delta)$.

In summary, the extension of the formula proposed by Roberts, which now takes into account thermal expansion and deviation from stoichiometry, is given by the set of Eqs. (10), (12), and (15).

It should be noted that the experimental imprecision associated with the determination of $\kappa_0(\delta)$ and α's (and, to a certain extent, $1-2|\delta|$), overwhelms the uncertainty associated with neglecting the higher-order terms in Eq. (9) and the approximation used to simplify Eq. (14) (namely, neglecting $\alpha_a^2\Delta T^2$ and $\alpha_a\alpha_c\Delta T^2$).

Setting $\delta=0$ (stoichiometric alloy) and assuming that thermal expansion is isotropic in the $L1_0$ structure [i.e., $\alpha_a(\delta) = \alpha_c(\delta)$], Roberts' formula [Eq. (1)] is recovered, in which the coefficient $\mathcal{B}$ corresponds to the term $1/\theta$ of Eq. (10). Therefore, in the original derivation by Roberts, it was implicitly assumed that thermal expansion is isotropic. However, because the $L1_0$ has a tetragonal symmetry, the thermal-expansion coefficients for the a and c parameters are not equal. As shown in Table I, $\alpha_a(\delta)$ and $\alpha_c(\delta)$ are very different from each other, especially for the case of CoPt and FePd $L1_0$ structures.

The relative importance of thermal expansion in Eq. (12) is controlled by $\alpha_\theta\Delta T$. As it can be seen from Eq. (15), α_θ increases with the anisotropy of the thermal expansion and with the c/a ratio. Using the lattice parameters presented in Fig. 2, we can estimate α_θ for the stoichiometric CoPt, NiPt, and FePd $L1_0$ alloys. The results obtained with a low-temperature reference of $T_0=300$ K are presented in Table I. The importance of thermal expansion is small for NiPt alloy but is appreciable for CoPt and FePd alloys. Indeed, at 800 K, the relative difference between the LROP predicted by the Roberts' formula and by the new one is 3% in NiPt, 10% in AuCu, 42% in CoPt, and 120% in FePd. These number underline the importance of considering the lattices thermal expansion and (their anisotropy) in the model. It can be appreciated that the value of α_θ for AuCu is relatively low, compared to CoPt or FePd, which might have explained the coherence of the results reported by Roberts in his original paper.[5]

TABLE I. a and c thermal-expansion coefficients of selected $L1_0$ tetragonal structures (Refs. 18–20). The corresponding parameter α_θ is computed using Eq. (15). All coefficients are given in 10^{-6} K^{-1} unit. The last line is the tetragonality ratio of the structures at 300 K.

Element	NiPt	CoPt	FePd	AuCu
α_a	15.0	22.2	54.2	18.8
α_c	11.1	−0.77	−33.8	−6.9
α_θ	61.	860.	2400.	196.
κ(300 K)	0.94	0.974	0.965	0.926

III. NUMERICAL APPROACH

The aim of the next sections is to test the accuracy of the model that we propose to relate the LROP to the tetragonality ratio. The present section details the numerical approach that we have used and the results are shown in the next section.

The stability of the $L1_0$ structure has been extensively studied using Ising models on a rigid fcc lattice with short-range interactions. These studies have mainly focused on the determination of the phase diagram and on the thermodynamical behavior of $L1_0$ domains (see Refs. 21 and 22, and references therein). However, thermal expansion of the lattice is obviously not taken into account in such models. We have therefore opted for a more realistic approach, albeit more computationally intensive, allowing continuous displacements of atoms.

To reach equilibrium, we have performed Monte Carlo simulations which take into account chemical as well as relaxation effects. The main advantage of Monte Carlo simulations is that when provided with the interatomic potential, the method is, in principle, exact. In particular, anharmonic effects (required to account for thermal expansion) and chemical correlations (necessary to accurately describe ordering) are taken into account. We used the simulations as numerical experiments in order to compute the relevant quantities with a good accuracy and perform systematics.

The calculations were performed with periodic boundary conditions at null pressure. Trials were of three kinds: random displacements of atoms, exchanges between two randomly chosen atoms, and a box expansion in the three orthogonal directions. The acceptance of the trials was based on the standard Metropolis algorithm.[23] In the Monte Carlo code, the main loop contained $(N_{disp}+N_{exch}+N_{exp})\times N_{atoms}$ trials of displacements, exchanges, and expansion. Typical values were $N_{disp}=10$, $N_{exch}=10$, and $N_{exp}=5$. The main loop

TABLE II. Modified Lennard-Jones potential parameters of Eq. (16). The lattice parameter of the pure B component is 5% larger than the one of the pure A component.

	A-A	A-B	B-B
ε(eV)	0.2	0.25	0.2
$\sigma^{\alpha\beta}$(Å)	2.4150	2.3738	2.2879
$p^{\alpha\beta}$	6	7.2920	6

was iterated until the system converged to equilibrium. We used a modified Lennard-Jones interatomic pair potential which stabilizes the $L1_0$ phase,[24]

$$V_{ij}^{\alpha\beta}(r_{ij}) = -4\varepsilon^{\alpha\beta}\left[\left(\frac{\sigma^{\alpha\beta}}{r_{ij}}\right)^{p^{\alpha\beta}} - \left(\frac{\sigma^{\alpha\beta}}{r_{ij}}\right)^{2p^{\alpha\beta}}\right], \quad (16)$$

where α and β stand for A or B. The cutoff on the interaction potential in Eq. (16) was set to 4.2 Å (i.e., between second and third nearest neighbors). In order to avoid discontinuities at the cutoff, a polynomial tapering function was used to smoothly decrease the potential to zero over 0.2 Å before the cutoff distance. We chose the melting temperature and the lattice parameter as fitting parameters in order to determine the quantities $\varepsilon^{\alpha\alpha}$ and $\sigma^{\alpha\alpha}$ for the pure crystals using a standard Lennard-Jones 6–12 potential (see Table II). Furthermore, a 5% lattice mismatch was imposed between the pure A and pure B fcc crystals. Finally, the cross parameters $\varepsilon^{\alpha\beta}$, $\sigma^{\alpha\beta}$, and $p^{\alpha\beta}$ were chosen so as to stabilize the $L1_2$ (AB_3) phase at null temperature and to reproduce the order-disorder transformation temperature close to 850 K.

Figure 3 represents a section of the calculated coherent composition-temperature phase diagram.[24] The diagram is characterized by a fcc solid solution at high temperature, and by single- and two-phase domains associated with the ordered structures $L1_2$ (AB_3), $L1_0$ (AB), and $L1_2$ (A_3B) at lower temperatures. This topology is typical of many systems exhibiting ordering on a fcc lattice such as CoPt, NiPt, FePt, and CuAu. The phase diagram was calculated in the $(N,\Delta\mu,P,T)$ semigrand canonical ensemble,[25] where $\Delta\mu$ is the difference between the chemical potentials of Co and Pt atoms. The simulation box contained $N_{atoms}=2048$ atoms. To reduce hysteresis effects, the initial configuration of each simulation box was divided in a slice of ordered phase and a slice of solid solution. The phase of the ordered part was chosen among the possible ordered phases [$L1_2$ (AB_3), $L1_0$ (AB), or $L1_2$ (A_3B)] with respect to the probed part of the phase diagram. Once convergence achieved, only single phases remained in the simulation box: ordered structures for $T<T^*$ and solid solutions for $T>T^*$.

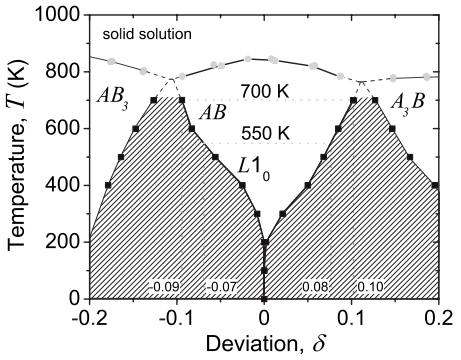

FIG. 3. Coherent phase diagram computed using the Monte Carlo method (see text for details). Two-phase regions are hatched. Dotted segments of phase boundaries are interpolated. The two-phase stability regions between the solid solution and the ordered phase are located along the gray circles. The extension of these regions is smaller than the accuracy of the calculations (5 K in temperature and 0.01 in composition).

The calculation of the lattice parameters and the LROP was realized in the (N,P,T) canonical ensemble. In the initial configurations, atoms were placed on a perfect fcc lattice of $16\times16\times16$ conventional unit cells. On a given site, the chemical nature of the atom was either chosen at random for temperatures above the transition temperature, or according to a $L1_0$ ordering, below the transition temperature. The selection of the compositions and the temperature ranges of the simulations was assisted by the calculated phase diagram. The simulations were performed between 300 and 930 K for an $A_{1/2+\delta}B_{1/2-\delta}$ alloy with $\delta=0$ and $\delta=0.05$. A series of simulations was also performed at 550 and 700 K with δ spanning across the single-phase region of the $L1_0$ phase (δ varied from −0.05 to 0.05 and from −0.08 to 0.08, respectively). Typically 3000 Monte Carlo loops were needed to reach the equilibrium. Once the equilibrium was reached, simulations continued for at least 2×10^5 loops.

Using an automated procedure, the lattice constants, the average compositions of (002) planes (C^α and C^β), and the atomic pair probabilities (P_{ij}^α, P_{ij}^β, and $P_{ij}^{\alpha\beta}$) were extracted from the atomic configurations at every 200 Monte Carlo loops. The equilibrium value of these quantities was then estimated by an average over at least 1000 of these configurations. Finally, the equilibrium LROP of the simulation η_{MC} was computed using Eq. (A2).

With a simulation box containing 16 384 atoms, the statistical precision of a quantity at equilibrium is estimated by the standard deviation of the stochastic variable defined as the average of the quantity over ten successive configurations. We found a statistical precision better than 10^{-3} Å for the lattice parameters and better than 2×10^{-3} for the average compositions of (002) planes. The precision for the atomic pair probabilities depended on the type of atomic pairs and on temperature but was always found better than 3×10^{-3}.

IV. RESULTS

In this section, we use the model $L1_0$ alloy detailed in the previous section to test the accuracy of the proposed relationship between the LROP from the tetragonality ratio. This is achieved by measuring independently the lattice parameters, thermal expansion, and LROP using Monte Carlo simulations.

Figure 4 represents the variation in the lattice parameters and their ratio as a function of the temperature for $\delta=0$ and $\delta=0.05$. The first-order transition between the solid solution and the $L1_0$ phase is marked by the discontinuity around

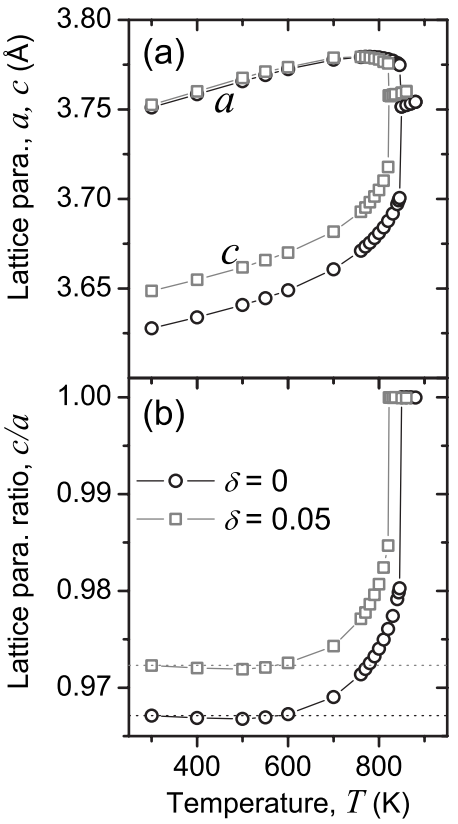

FIG. 4. Evolution of the lattice constants, (a) a and c and (b) the tetragonality ratio (c/a) with temperature for a simulated $L1_0$ stoichiometric alloy (○) and an alloy with a deviation from stoichiometry δ=0.05 (□). The dotted line in (b) is the c/a parameter at 300 K.

850 K. The minimum value of c/a is not found at the lowest temperature of 300 K but around 500 K. The trend shown by the Monte Carlo simulation is similar to the experimental data of NiPt, shown in Fig. 2(a).

As explained in Sec. II, an important quantity is the relative difference between the lattice expansion coefficients, $\alpha_a - \alpha_c$, measured at low temperature. Figure 5 shows the lattice expansion coefficients and their relative difference de-

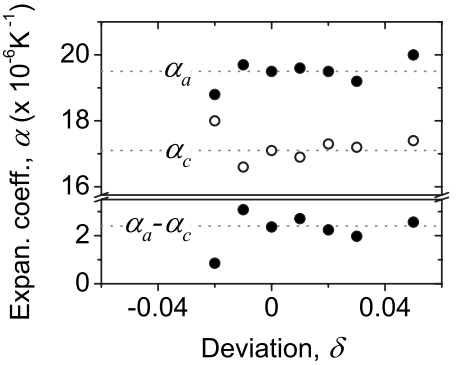

FIG. 5. a and c lattice expansion coefficients and their difference, $\alpha_a - \alpha_c$, at several deviations from stoichiometry δ, deduced from the simulations performed at 300 and 400 K. The dotted lines mark the average value.

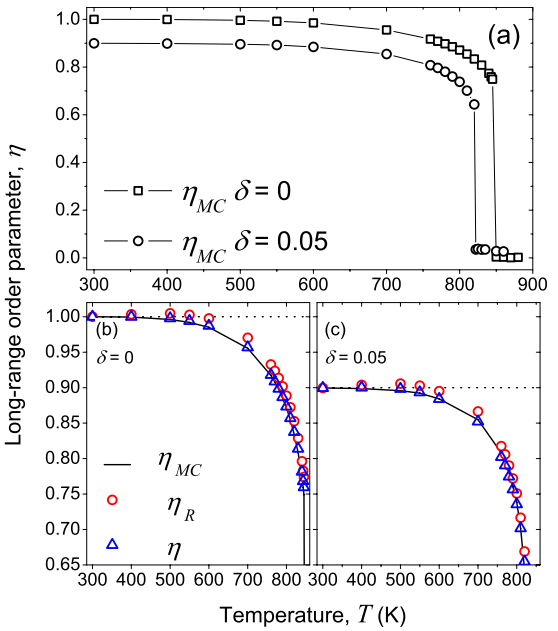

FIG. 6. (Color online) (a) Reference long-range order parameter deduced from the Monte Carlo simulations between 300 and 900 K for a stoichiometric alloy (□) and an alloy with a deviation from stoichiometry δ=0.05 (○). Portion of (a) between $0.65 < \eta < 1$. η_{MC} (black line) is the reference LROP computed from the atomic configurations, η_R is the estimation using Roberts formula (○), and η is the improved estimation obtained with Eqs. (10), (12), and (15) (△). Computed for a stoichiometric alloy, δ=0 (b), and an alloy with a deviation from stoichiometry δ=0.05 (c).

duced from the computed lattice parameters at 300 and 400 K. Note that, within the 300–400 K temperature range, the order parameter is equal to its maximum value with a precision better than 4×10^{-4} (see Fig. 4). Therefore, the only contribution to the change in the lattice constants with temperature is thermal expansion.

As it can be appreciated from Fig. 5, the thermal expansion is anisotropic because α_a is about 15% higher than α_c. However, the statistical precision on the measurement of the lattice-parameter expansion is limited because the lattice-parameter variation between the 300 and 400 K is on the order of 2×10^{-3} Å, i.e., only slightly above the statistical precision of the lattice-parameter measurement (about 10^{-3} Å, see Sec. III). Therefore, we assumed that the scatter in Fig. 5 of the values of the expansion coefficients with δ around a mean value (dotted line) is random. For all practical purpose, we considered that the thermal-expansion coefficients are constant with respect to δ in the concentration range $-0.06 < \delta < +0.06$, and we have used the values $\alpha_a = 19.5 \times 10^{-6}$ K^{-1}, $\alpha_c = 17.1 \times 10^{-6}$ K^{-1}, and $\alpha_a - \alpha_c = 2.4 \times 10^{-6}$ K^{-1} with a corresponding standard deviation (estimated from the values given in Fig. 5) of 0.5×10^{-6} K^{-1}. Increasing the accuracy by an order of magnitude would have required unaffordable computation times.

The equilibrium values of the order parameter as a function of temperature were extracted from the Monte Carlo simulations. These results are presented in Fig. 6 for δ=0 and δ=0.05. As expected, the LROP reaches its maximal value, $1 - 2|\delta|$, at low temperature. The LROP continuously

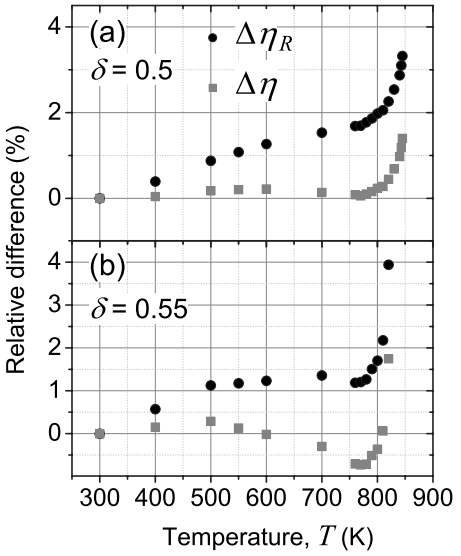

FIG. 7. Relative difference, Δ, between Roberts' estimate of the LROP, η_R [●, Eq. (1)], and the proposed equation, η [■, Eqs. (10), (12), and (15)] with respect to the LROP deduced from the Monte Carlo simulations (η_{MC}). The relative differences are plotted for simulations performed at various temperatures for two nominal compositions: (a) δ=0 and (b) 0.05.

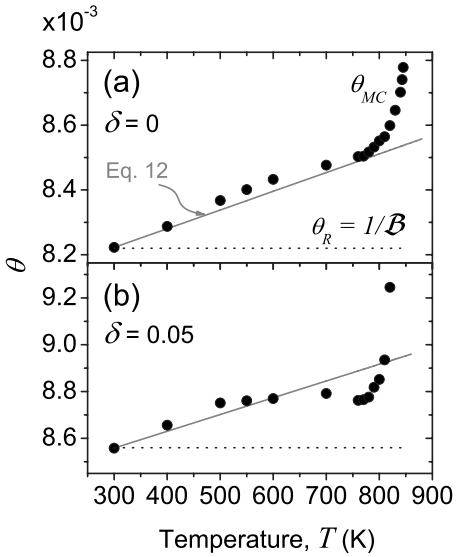

FIG. 8. θ parameter as a function of temperature [black line, Eq. (12)] compared to the value deduced from the Monte Carlo simulations (θ_{MC}, ●) at various simulated temperatures for alloys with (a) δ=0 and (b) δ=0.05. The constant $\theta_R = 1/\mathcal{B}$, with $\mathcal{B}$ defined in Eq. (1) is displayed as a dotted line for comparison.

decreases with temperature up to the transition temperature, T^*, at which the LROP abruptly falls to zero. For a stoichiometric alloy, T^*=845 K and the critical value of the LROP, η^* is close to 0.75. For δ=0.05, a slightly lower T^* is achieved, at T^*=820 K with a corresponding η^* close to 0.64, consistent with the phase diagram shown in Fig. 3. The large value of the critical LROP indicates that the character of the transition is largely assigned to a first-order type.[26]

Having measured independently the lattice parameters, thermal-expansion coefficients, and the LROP, the accuracy of the proposed formula to deduce the LROP from the value of the tetragonality ratio can be tested. Using the reference value at T=300 K and Eq. (1) we have computed η_R, the LROP predicted by Roberts' formula. Using the set of Eqs. (10), (12), and (15), we have computed the refined estimate η, which takes into account the anisotropy of thermal expansion. Figure 6 shows the variation in these quantities as a function of temperature for two compositions. First, as expected from the shape of the c/a curve, η_R has the important drawback to predict nonphysical values ($\eta_R > 1$) between 300 and 550 K. In addition, it is clear that the improved estimate, η, is in better agreement with the MC results than the values associated with Roberts' formula.

A more convenient figure of merit for the accuracy of the formula is the relative differences $\Delta\eta_R$ and $\Delta\eta$ (with respect to the reference LROP, η_{MC}). This difference is represented for the simulated temperatures in Fig. 7. For the stoichiometric composition [Fig. 7(a)], the curves are almost linear below $0.9T^*$(=775 K), followed by a sharp increase just below T^*. In the linear part, $\Delta\eta$ is very close to zero up to $0.9T^*$ whereas $\Delta\eta_R$ continuously increases with temperature up to 1.7%.

For the nonstoichiometric alloy [Fig. 7(b)], it is also observed that the relative error $\Delta\eta$ is very small below $0.9T^*$, corresponding to $0.9\eta_\delta$, (below 0.5%) whereas the error $\Delta\eta_R$ reaches 1.5%. As explained in Sec. II, the accuracy of Roberts' formula is not particularly unreasonable (below 2%) in this specific example only because the anisotropy of thermal expansion is small in the simulated $L1_0$ alloys.

Close to the transition temperature T^*, we observe a significant increase in $\Delta\eta_R$ and $\Delta\eta$, both in the case of the stoichiometric and nonstoichiometric alloys. Albeit the reasonable accuracy of η (~0.5% and 2% for δ=0 and 0.05, respectively), it is important to understand the origin of this behavior, in order to evaluate its importance in real alloys. It will be shown in the discussion that this behavior is due to the inaccuracy of the mean-field approximation used to evaluate the pair probability functions.

Let us recall from Sec. II, that Roberts' formula and our refined model are both based on Eq. (10) and differ by the value of the prefactor θ. In Roberts' formalism, $\theta_R = 1/\mathcal{B}$ is temperature independent whereas in our extended formula, θ evolves linearly with temperature [see Eq. (12)]. It is thus interesting to compute the exact value of the prefactor θ_{MC}, obtained using Eq. (10), in which the values of the LROP η_{MC} and the tetragonality ratio measured in the Monte Carlo simulations are introduced.

θ_{MC}, θ_R, and θ are compared in Fig. 8. For the stoichiometric alloy (δ=0), θ_{MC} is an increasing function of temperature. The positive slope of the linear increase is not taken into account in Roberts' approach and therefore the accuracy of Roberts' formula decreases with temperature. In comparison, in our revised formula, a linear dependence of θ is taken into account and leads to a good agreement with θ_{MC} below $0.9T^*$. For the out-of-stoichiometry (δ=0.05) alloy, the same trend is observed albeit a poorer agreement.

The marked increase in θ_{MC} near the transition temperature, T^*, demonstrates that our linear approximation is no longer sufficient. A detailed analysis of the validity of the

TABLE III. Probability of finding atom A or B in neighboring sites i or j within A-rich (002) planes, P_{ij}^{α} and B-rich 002 planes, P_{ij}^{β} and between (002) planes, $P_{ij}^{\alpha\beta}$.

Position		Within (002) planes			Between (002) planes
i	j	P_{ij}^{α}	P_{ij}^{β}	Average, $\frac{1}{2}(P_{ij}^{\alpha}+P_{ij}^{\beta})$	$P_{ij}^{\alpha\beta}$
A	A	$(C^{\alpha})^2$	$(C^{\beta})^2$	$\frac{1}{2}[(C^{\alpha})^2+(C^{\beta})^2]$	$C^{\alpha}C^{\beta}$
B	B	$(1-C^{\alpha})^2$	$(1-C^{\beta})^2$	$\frac{1}{2}[(1-C^{\alpha})^2+(1-C^{\beta})^2]$	$(1-C^{\alpha})(1-C^{\beta})$
A	B	$C^{\alpha}(1-C^{\alpha})$	$C^{\beta}(1-C^{\beta})$	$C^{\alpha}(1-C^{\alpha})+C^{\beta}(1-C^{\beta})$	$C^{\alpha}(1-C^{\beta})+(1-C^{\alpha})C^{\beta}$
B	A	$(1-C^{\alpha})C^{\alpha}$	$(1-C^{\beta})C^{\beta}$		

assumptions subtending our refined formula is necessary to identify and explain the cause of this discrepancy close to T^*. This analysis is performed in the next section.

V. DISCUSSION

The Monte Carlo simulation results presented in the previous section have shown that the proposed extension of the Roberts' formula quantitatively improves the description of the relationship between the long-range order parameter and the c/a ratio for stoichiometric and nonstoichiometric alloys up to about $T=0.9T^*$. In other words, we have shown that the thermal-expansion coefficients of the crystal must be taken into account in the data analysis. However, our extension of Roberts' approach is unable to accurately reproduce the behavior of the LROP and the c/a ratio for temperatures very close to T^*, typically in the $0.9T^*-T^*$ range which roughly corresponds to values of LROP in the range $0.9\eta_{\delta}-\eta_{\delta}$. From the derivation of the Roberts' and modified Roberts' approaches, we could relate these discrepancies to the fact that both approaches (i) are based on a mean-field approximation, known to poorly describe the thermodynamics close to $L1_0$ to fcc transition temperature and (ii) estimate the mean bond length (and therefore the lattice parameters) from the relative occurrence of each possible atomic pair. In the following, we first address these two assumptions and then we study the relation between the LROP and the tetragonality ratio close to the transition temperature using a Landau expansion.

A. Analysis of the mean-field approximation

As it was shown in Sec. II, Roberts' formula is based on a mean-field approximation derived from the occupancy probability of neighboring sites. It is possible to evaluate the range of validity of this assumption directly from the Monte Carlo simulations. From equilibrated Monte Carlo configurations, we have extracted the concentration of the atomic planes together with the paired occupancy, directly from counting atomic sites. The difference, W_{ij}, between the occupancy, as obtained directly from counting (Q_{ij}), and the occupancy probability, computed from the atomic plane concentration (P_{ij}, Table III), is a measure of the deviation from the mean-field approximation,

$$W_{ij}^{\alpha} = P_{ij}^{\alpha} - Q_{ij}^{\alpha},$$

$$W_{ij}^{\beta} = P_{ij}^{\beta} - Q_{ij}^{\beta},$$

$$W_{ij}^{\alpha\beta} = P_{ij}^{\alpha\beta} - Q_{ij}^{\alpha\beta}. \quad (17)$$

In Fig. 9, we have plotted a selection of W_{ij} parameters for a stoichiometric alloy. For low temperatures, the W_{ij} parameters are typically null, implying that the mean-field approximation is valid in these conditions. Indeed, antisites (α sites occupied by B atoms or β sites occupied by A atoms) become sufficiently diluted at low temperatures for their interaction to be minimal.

Close to the transition, the deviation from the mean-field approximation markedly increases. The largest values are found for the parameter $|W_{AB}^{\alpha\beta}|$, which suggests the appearance of a short-range order between α and β planes. When correlating the deviation of the calculated pair probability to the bias of the order parameter, it becomes apparent that, close to the transition point, the precision of Roberts' estimates is limited by the mean-field approximation.

The mean-field approximation is also tested for off-stoichiometric alloys by plotting the W_{ij} parameters for different values of the deviation from stoichiometry in Fig. 10. The results indicate a systematic deterioration of the mean-field approximation with increasing deviation from the equimolar composition. This can be easily understood by realizing that a deviation δ from stoichiometry implies the presence of antisites concentration above $2|\delta|$ in one type of planes. This is illustrated in Fig. 11 in which the compositions of both types of plane are plotted against the deviation from stoichiometry, at two temperatures. Each data set is

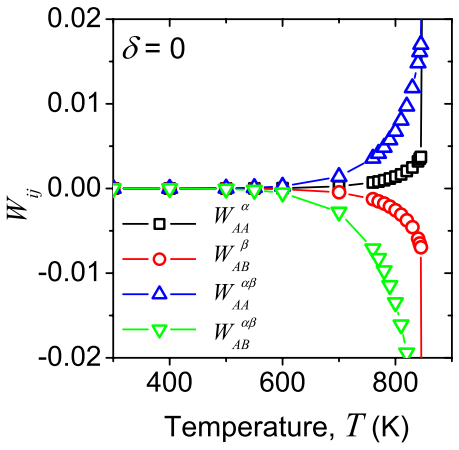

FIG. 9. (Color online) Selected W^{ij} parameters deduced from the simulations performed at various temperatures for a stoichiometric alloy (δ=0).

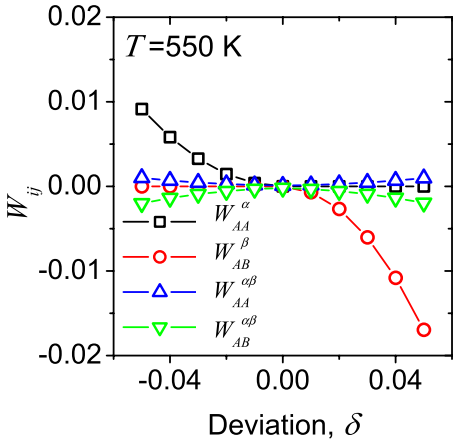

FIG. 10. (Color online) Selected W^{ij} parameters at 550 K as a function of the deviation from stoichiometry δ.

composed of two branches: the upper (lower) curves correspond to the concentration of $A(B)$-rich planes; with a positive (negative) deviation from stoichiometry. At 550 K, for $\delta>0$ the temperature is sufficiently low to saturate the α planes and for β planes to approach $2|\delta|$. At higher temperature (700 K), α planes become unsaturated and the content of β planes deviates from the $2|\delta|$ slope as a result of thermal fluctuations. Therefore, the precision of the mean-field approximation will depreciate with the combined consequence of thermal fluctuations and deviation from stoichiometry.

B. Analysis of the underlying energetic model

Our extension of Roberts' formula is derived from the same premises formulated by Roberts, which are based on the number and length of nearest-neighbor bonds in the $L1_0$ structure. This hypothesis encompasses the necessary physics in order to relate the c/a ratio to the order parameter. However, this approach can only be quantitatively justified within a simple energetic framework in which the atomic interaction is modeled by considering that nearest neighbors are connected by springs with identical constants. Using this simplified model, it is thus possible to extract some trends

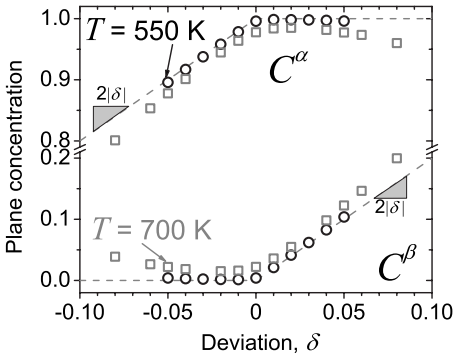

FIG. 11. Average (002) planes composition (C^{α} and C^{β}) deduced from simulations performed for various nominal compositions at 550 K (○) and 700 K (□). The dashed lines are calculated using Eq. (2) with $\eta=0$.

but quantitative predictions must be considered with circumspection.

Quantitative limits to the model are immediately apparent when comparing the lattice parameters, (a,c) of the stoichiometric $L1_0$ structure with lattice constants of the constituents, a_A and a_B. Indeed, at low temperature, T_0, the model predicts the following relationship for the lattice constants:

$$a = \frac{(a_A + a_B)}{2}$$

and for the thermal-expansion coefficients,

$$\alpha_a a = \frac{(\alpha_A a_A + \alpha_B a_B)}{2}.$$

However, a mismatch is present when comparing the mean of the lattice constants of the pure constituents with that of the $L1_0$ structure. For example, if we calibrate the characteristic lengths, $\ell_{AA}(T_0)$ and $\ell_{BB}(T_0)$ on the lattice constants of the pure constituents at low temperature, T_0, the calculated mismatch is 0.7% for our Lennard-Jones model, 2.5% and 3% for the NiPt and CuAu $L1_0$ structures, respectively. It is shown (in Appendix) that this bias is obvious when comparing the lattice constants at different deviations from stoichiometry (as deduced from the knowledge of the three characteristic lengths) with the reference lattice constants (as computed by Monte Carlo methods).

Additionally, a simplifying hypothesis was implied: it was assumed that the atomic positions coincide with the lattice sites of the structure. This type of approximation was also invoked for the study of Vegard's law at the atomic scale.[27] However, owing to the intrinsic difference between the atomic radius of the constituents, local distortions can occur in the crystal and shift the mean position of the atoms with respect to the crystal sites.[28]

In light of these arguments, it would appear that the method proposed by Roberts is unsuitable for obtaining a high-precision relation between the c/a ratio and the order parameter. Therefore, it can be surprising that our modified Roberts formula is capable of obtaining order parameters with such a remarkable precision. This can be justified from the fact that the modified Roberts formula can also be derived using a Landau-type expansion, which will be made explicit in the following.

C. Landau-type expansion

The relation between the LROP and the lattice parameters of the $L1_0$ structure can be derived using a Landau-type expansion, similar to those used to study phase transitions in ferroelectrics.[29] This approach consists of taking a polynomial expansion of the excess Gibbs free energy with respect to the disordered phase for which the LROP η and the spontaneous strain ϵ_{ij} are zero. With this approach, we implicitly conjecture that only the average concentration and the LROP (or equivalently, only the planes concentration, C^{α} and C^{β}) are sufficient to determine the lattice constants. The corollary is to assume a homogeneous distribution of A and B atoms within α and β planes. For small deviations from stoichiom-

etry, this approximation is valid at low temperatures, owing to the diluted level of the minor constituent within each type of planes; these atoms can be considered isolated from each other. For higher temperatures, this assumption implies neglecting the influence of the short-range order.

Landau-type expansions were initially developed to study second-order transitions whereas the transition considered here is of the first order. The drawback of the Landau approach, when considering second-order transitions, is that the long-wavelength fluctuations, which are important to accurately describe the transition, are ignored. In the case of first-order transitions, the wavelength of the fluctuations does not diverge at the transition, making the Landau approach better suited. Landau-type expansions have been successfully applied to describe first-order transitions in a semiquantitative way.[30] In that case, the description of the excess Gibbs free energy as a polynomial expansion was a convenient way of constructing a functional fulfilling the necessary requirements dictated by the system (symmetries, equilibrium values, etc.).[31,32] Therefore, provided an accurate expansion, this approach is not limited to the description of the transition but is valid over a large range of temperature. Taking due account of the symmetries, the excess Gibbs free energy $\Delta G(T,P,c,\eta,\varepsilon_{ij})$ of a homogeneous $L1_0$ phase is

$$\Delta G = \left[\frac{1}{2}\tilde{A}\eta^2 - \frac{1}{4}\tilde{B}\eta^4 + \frac{1}{6}\tilde{C}\eta^6 + \cdots\right] + \left[\frac{1}{2}\lambda_{ijkl}\epsilon_{ij}\epsilon_{kl}\right] + [\eta^2\xi_{ij}\epsilon_{ij} + \cdots]. \tag{18}$$

The above expression consists of three terms. The first is the Landau potential $f_L(\eta,T)$ which depends both on temperature and the LROP η. An expansion up to the sixth order of η is necessary to reproduce the first-order transition but the potential can be expanded to a higher order, if the details of a complex energy landscape needs to be reproduced. In this expansion, the parameters $\tilde{A}$, $\tilde{B}$, … are temperature dependent. $\tilde{A}$ changes sign at a temperature close to the transition temperature and is assumed to evolve linearly with temperature. However, a more complex form of $\tilde{A}$ is necessary for reproducing the low-temperature behavior of the order parameter.[33]

The second term of Eq. (18) is the elastic energy resulting from the relaxation of the unit cell described by the spontaneous strain ϵ_{ij}. The λ_{ijkl} refer to the elastic constants of the fcc disordered phase. The last term is the interaction energy between the LROP and the spontaneous strain. With a proper choice of the Landau potential $f_L(\eta,T)$, expression (18) is valid for all η, but only for small strains, because it relies on the theory of linear elasticity. Finally, note that all the coefficients of the expansion, i.e., $\tilde{A}$, $\tilde{B}$, $\tilde{C}$, λ_{ijkl}, and ξ_{ij} may depend on concentration, temperature, and pressure.

Following the fcc$\rightarrow L1_0$ transition with a tetragonal axis along z, the spontaneous strain becomes diagonal,

$$(\epsilon_{ij}) = \begin{pmatrix} \epsilon_1 & 0 & 0 \\ 0 & \epsilon_1 & 0 \\ 0 & 0 & \epsilon_3 \end{pmatrix}. \tag{19}$$

The expansion in Eq. (18) becomes, to the lowest order,

$$\Delta G = \left[\frac{1}{2}\tilde{A}(T-T_1)\eta^2 - \frac{1}{4}\tilde{B}\eta^4 + \frac{1}{6}\tilde{C}\eta^6\right] + \left[C_{11}\left(\epsilon_1^2 + \frac{\epsilon_3^2}{2}\right) + C_{12}(\epsilon_1^2 + 2\epsilon_1\epsilon_3)\right] + \eta^2[2\xi_1\epsilon_1 + \xi_3\epsilon_3], \tag{20}$$

where we have used the Voigt notations for the elastic constants and where the coupling terms ξ_1 and ξ_3 are equal to ξ_{11} and ξ_{33}, respectively.

Writing the condition of equilibrium with respect to the spontaneous strain, $\frac{\partial \Delta G}{\partial \epsilon_i} = 0$ and solving these equations leads to

$$\epsilon_1 - \epsilon_3 = \Lambda_S\eta^2 \quad 2\epsilon_1 + \epsilon_3 = \Lambda_V\eta^2, \tag{21}$$

where $\Lambda_S(T,P,c)$ and $\Lambda_V(T,P,c)$ are defined by

$$\Lambda_S = \frac{\xi_3 - \xi_1}{C_{11} - C_{12}}, \tag{22a}$$

$$\Lambda_V = -\frac{2\xi_1 + \xi_3}{C_{11} + 2C_{12}}. \tag{22b}$$

Λ_S and Λ_V are the coefficients directly related to the shape and volume changes, respectively.

From Eq. (21), it is obvious that the spontaneous strain evolves quadratically with the LROP. We can now relate the LROP to the lattice parameters using the definition of the spontaneous strain components, at a given temperature T below the $L1_0$-fcc transition temperature, T^*,

$$\epsilon_1 = \frac{a(T) - a_{\mathrm{fcc}}(T)}{a_{\mathrm{fcc}}(T)} \quad \epsilon_3 = \frac{c(T) - a_{\mathrm{fcc}}(T)}{a_{\mathrm{fcc}}(T)}, \tag{23}$$

where $a(T)$ and $c(T)$ are the lattice parameters of the $L1_0$ structure and $a_{\mathrm{fcc}}(T)$ is the extrapolation of the lattice parameter of the fcc solid solution at temperature T. As detailed in Ref. 29, the extrapolation of the lattice parameters of the high-symmetry phase over a large temperature interval of the low-symmetry phase requires a good knowledge of the thermal expansion of the high-symmetry phase.

Using Eqs. (21) and (23), we can relate the tetragonality ratio κ to the LROP,

$$1 - \kappa = \frac{\epsilon_1 - \epsilon_3}{1 + \epsilon_1} = \frac{\Lambda_S\eta^2}{1 + \frac{1}{3}(\Lambda_S + \Lambda_V)\eta^2}. \tag{24}$$

Because the strains are small, the above expression can be expanded as

$$1 - \kappa = \Lambda_S\eta^2\left[1 - \frac{1}{3}(\Lambda_S + \Lambda_V)\eta^2\right] + \cdots. \tag{25}$$

Retaining the first term of the expansion, a linear relationship between the tetragonality ratio and the square of the LROP is obtained,

$$1 - \kappa = \Lambda_S(\delta,T)\eta^2. \tag{26}$$

It is important to stress that the accuracy of the above expansion is related to the value of the strain ϵ_1. The strain ϵ_1 is usually close to 1% [$\epsilon_1 \approx 0.6\%$ in CoPt,[18] 1% in FePd,[19] and

2% in NiPt (Ref. 18)]. Therefore, if the coefficient $\Lambda_S(\delta,T)$ is known, Eq. (26) has the ability to predict the value of the LROP with an accuracy on the order of 1%.

Unfortunately, it appears that this relationship is, at this point, unusable from an experimental perspective because the coupling parameters ξ_1 and ξ_3, and therefore the coefficient $\Lambda_S(\delta,T)$, are not known. To estimate the value of $\Lambda_S(\delta,T)$, we proceed as in Sec. IV, and use the low-temperature behavior of Eq. (26). At a temperature typically lower than $T^*/2$, the LROP approaches η_δ, and the temperature variations in the lattice parameters are strictly the result of thermal expansion. Because thermal expansion is linear, we obtain, at low temperatures, a linear variation between the prefactor and the temperature. Assuming that this linear behavior still holds at higher temperatures, Eqs. (12) and (15) are deduced and the extension of Roberts' formula is retrieved (which takes into account the lattices thermal expansion and the deviation from stoichiometry). Therefore, the proposed treatment allows the extension of Roberts' formulas without making the assumptions of a simplified energetic model based on spring interactions between atoms.

The evaluation of the coefficient $\Lambda_S(\delta,T)$ using a low-temperature expansion makes the formula perfectly accurate at low temperatures. When increasing temperature, the accuracy of the formula slightly decreases for two reasons. First, according to Eq. (26), changing $1-c/a$ by x modifies η^2 by $\Lambda_S(\delta,T)x$. As shown by the above Landau expansion, this relationship is accurate to $\sim 1\%$. This leads to a very small error on the value of the LROP, on the order of $x/100$. Second, the Landau expansion, in the same way as the Roberts' original derivation, does not explicitly take into account the short-range order, which can be significant close to the transition temperature, if the transition is not of a strong first-order character, as discussed in Sec. V A.

D. Practical considerations

The proposed extension of Roberts' formula using Eqs. (10), (12), and (15) relates the LROP of an alloy to the c/a ratio obtained by x-ray diffraction patterns of a bulk homogeneous alloy, conveniently avoiding the consideration of the polarization factor, absorption correction, the Debye-temperature factor, etc.[34] The added precision of our formulas is obtained at the cost of collecting, the low-temperature lattice constants and corresponding linear-expansion coefficients [α_a and α_c, in Eq. (13)] of the alloy at the concentration of interest. However, these are parameters that are naturally and easily accessible with a high level of precision from the standard analysis of two or three powder-diffraction patterns obtained at different temperatures, typically below $T^*/2$. The precise knowledge of these quantities is essential for the accurate estimate of the LROP from the values of the c/a deduced from the powder-diffraction patterns obtained at temperatures between $T^*/2$ and the temperature corresponding to $0.9\eta_\delta$. Between the temperature corresponding to $0.9\eta_\delta$ and T^*, a loss of accuracy of our method in computing the LROP should be expected with increasing temperature.

The proposed method also implies that the lattice expansion coefficients deduced from low-temperature experiments are still valid at higher temperatures in the range of interest. It is obviously not possible to verify experimentally the validity of this extrapolation for $L1_0$ structure owing to the fact that the variation in the lattice constants with temperature will also be function of ordered-induced phenomena.

Roberts' relation and the set of Eqs. (10), (12), and (15) are both subjected to the physical constraints of the material being probed. In particular, we have considered a stress-free $L1_0$ alloy, for which we have shown that the c/a ratio can be determined from the composition of the (002) planes and the lattice expansion coefficients. It is well known, however, that local strain can also affect the lattice constants and bias the c/a ratio, especially when texture is present. In these circumstances, Roberts' formula or our modified version should be used with caution.

Strain can result in the presence of backstresses, dislocations, stacking faults, voids, etc., and other microstructural defects. Local strain can arise from free surfaces, interface with second phases or size-induced phenomena. In order to use Roberts' formula or the modified version, it is therefore necessary to measure the occurrence of these microstructural aspects in the alloy and assess their influence on the lattice tetragonality. In this context, it would be hazardous to use the proposed equation as well as Roberts' equation for thin films, nanostructured alloys, or heavily damaged materials, for example.

VI. CONCLUSION

In this paper, we propose an extension of Roberts' formula in order to accurately compute the long-range order parameter from the measured tetragonality ratio of bulk $L1_0$ alloys. The new version of the equation takes into account the thermal lattice expansion and the deviation from the stoichiometric concentration. In particular, we demonstrate that the anisotropy of the thermal lattice expansion in $L1_0$ alloys is an important parameter for relating the value of the long-range order parameter to the tetragonality ratio. This formula lends itself to typical *in situ* x-ray diffraction studies in which an accurate measurement of the long-range order parameter is required.

To test the accuracy of the proposed formula and the validity of the underlying assumptions, we used Monte Carlo simulations with a Lennard-Jones position-dependent pair potential. In the simulations, we have measured independently the long-range order parameter and the tetragonality ratio as a function of temperature. The simulation results show that, even for alloys having a small anisotropy of the thermal lattice expansion (i.e., around 15%), the proposed formula is significantly more accurate than Roberts' equation. We pointed out that the single-site mean-field approximation used to derive the formula breaks down with a high concentration of the minor element in the (002) planes. This occurs near the transition point (typically for a LROP lower than 0.9 times its maximum value) and for large deviations from stoichiometry.

The formalism presented here could be easily extended to alloys exhibiting other types of first-order ordering transition such as $L1_1$ structures. For example, CuPt exhibits a first-

order cubic to rhombohedral ordering transformation. The LROP in CuPt can be conveniently related to the rhombohedral angle via a relation deduced using a nearest-neighbor sites within and between (111) planes. The correction presented in this paper could be easily extended to the relation proposed by Ref. 35 in order to take into account the lattice expansion and extend the relation to alloys displaying deviation from stoichiometries.

ACKNOWLEDGMENTS

We wish to express our gratitude to A. Finel for very helpful discussions. We acknowledge the Natural Sciences and Engineering Research Council of Canada for funding and the French National Agency for Research (ANR) for supporting this work.

APPENDIX: DEMONSTRATIONS

1. Demonstration of Eq. (4)

Consider an ordered $A_{1/2+\delta}B_{1/2-\delta}$, $L1_0$ structure which admits a deviation from stoichiometry δ. Let C^α and C^β, the concentration of A atoms in two successive (002) planes, with α and β planes being rich in A and B atoms, respectively. δ is simply related to the average of C_α and C_β,

$$\delta = \frac{C^\alpha + C^\beta}{2} - \frac{1}{2}. \tag{A1}$$

We define the order parameter η as

$$\eta = C^\alpha - C^\beta, \tag{A2}$$

which are equivalent to Eq. (2). From these definitions, identities are derived,

$$C^\alpha + C^\beta = 2\delta + 1, \tag{A3a}$$

$$2C^\alpha C^\beta = 2\left(\delta + \frac{1}{2}\right)^2 - \frac{\eta^2}{2}, \tag{A3b}$$

$$(C^\alpha)^2 + (C^\beta)^2 = 2\left(\delta + \frac{1}{2}\right)^2 + \frac{\eta^2}{2}. \tag{A3c}$$

These identities are useful for deriving the pair probabilities referred to in Eq. (3), within the single-site mean-field approximation. Table III lists all possible pair probabilities and are written in terms of C^α and C^β. Within A- or B-rich (002) planes, the probabilities are expressed as P_{ij}^α and P_{ij}^β, respectively, and between (002) planes, they are referred to as $P_{ij}^{\alpha\beta}$. One can verify that the coefficients P_{ij} sum to unity in each column of Table III.

Inserting the terms of Table III in Eq. (3) and using the identities listed in Eq. (A3) to express the characteristic lengths in terms of δ and η yields

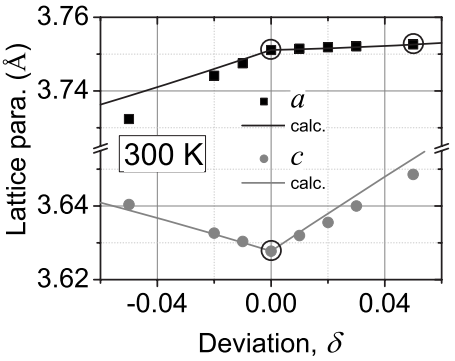

FIG. 12. a (■) and c (●) lattice constants averaged over the entire Monte Carlo cell simulated with deviation from stoichiometry selected between δ=−0.05 to 0.05 at 300 K. The solid lines were computed from the encircled data points using method described in Appendix Eq. (A5).

$$\bar{\ell}_1 = \frac{a}{\sqrt{2}} = \ell(\delta) + \frac{\eta^2}{4}\mathcal{L}^-, \tag{A4a}$$

$$\bar{\ell}_2 = \frac{a}{\sqrt{2K}} = \ell(\delta) - \frac{\eta^2}{4}\mathcal{L}^-, \tag{A4b}$$

in which $\ell(\delta)$ and $\mathcal{L}^-$ are defined in Eq. (5).

Dividing Eq. (A4b) by Eq. (A4a) yields Eq. (4), from which Eq. (7) is derived by isolating η.

2. Evolution of the lattice parameter with composition

Using Eq. (A4), it is possible to deduce the variation in the lattice constants at low temperature with the composition, $a_0(\delta)$ and $c_0(\delta)$, knowing the three characteristic bond lengths, $\ell_{ij}0$, at the low-temperature reference, T_0,

$$a_0(\delta) = \sqrt{2}\bar{\ell}_1^0, \tag{A5a}$$

$$c_0(\delta) = \sqrt{4\bar{\ell}_2^{02} - 2\bar{\ell}_1^{02}}. \tag{A5b}$$

Experimentally, as shown in Fig. 12, $a_0(\delta)$ and $c_0(\delta)$ can be plotted numerically using Eq. (A5) from three values of either lattice constant, at a known stoichiometry (for example, the values of $a_0(0)$, $c_0(0)$, and say, $a_0(0.05)$, as it was done to generate de full lines in Fig. 12).

The shift between the curves in Fig. 12 and the simulated data points found at large deviation from stoichiometries highlights the bias introduced by the single-site mean-field approximation.

3. Linearity of θ with T

By considering the linear expansion of the characteristic lengths, ℓ_{ij}, it is possible to demonstrate that θ, in Eq. (8),

$$\theta(\delta) = \frac{4\mathcal{L}^-}{\ell(\delta)} \tag{A6}$$

can be considered linear with temperature. We start byexpressing the characteristic lengths as linear functions of temperature,

$$\ell_{ij} = \ell_{ij}^0(1 + \alpha_{ij}\Delta T) \tag{A7}$$

with $\Delta T = T - T_0$, where T_0 is the low-temperature reference, α_{ij} is the corresponding linear-expansion coefficient of the ℓ_{ij} bond, and ℓ_{ij}^0 is the bond length at T_0.

We can rewrite $\mathcal{L}^+$ and $\mathcal{L}^-$, defined in Eq. (5) using Eq. (A7),

$$\mathcal{L}^- = \mathcal{L}_0^-(1 + \Lambda^-\Delta T), \tag{A8a}$$

$$\mathcal{L}^+ = \mathcal{L}_0^+(1 + \Lambda^+\Delta T), \tag{A8b}$$

$$\ell(\delta) = \ell_0(\delta)[1 + \zeta(\delta)\Delta T], \tag{A8c}$$

in which

$$\Lambda^- = \frac{\ell_{AA}^0\alpha_{AA} + \ell_{BB}^0\alpha_{BB} + 2\ell_{AB}^0\alpha_{AB}}{\mathcal{L}_0^-}, \tag{A9a}$$

$$\Lambda^+ = \frac{\ell_{AA}^0\alpha_{AA} + \ell_{BB}^0\alpha_{BB} - 2\ell_{AB}^0\alpha_{AB}}{\mathcal{L}_0^+}, \tag{A9b}$$

$$\zeta(\delta) = \frac{1}{\ell_0(\delta)}[\Lambda^+\mathcal{L}_0^+ + (\ell_{AA}^0\alpha_{AA} + \ell_{BB}^0\alpha_{BB})\delta + \Lambda^-\mathcal{L}_0^-\delta^2]. \tag{A9c}$$

The superscript or underscript "0" refers to the quantity evaluated at the reference temperature, T_0.

Inserting Eq. (A8) in Eq. (A6) yields

$$\theta(\delta) = \frac{1}{4}\frac{\mathcal{L}_0^-(1 + \Lambda^-\Delta T)}{\ell_0(\delta)(1 + \zeta(\delta)\Delta T)} \tag{A10a}$$

$$\approx \frac{\mathcal{L}_0^-}{4\ell_0(\delta)}(1 + \Lambda^-\Delta T)(1 - \zeta(\delta)\Delta T) \tag{A10b}$$

$$\approx \theta_0(\delta)[1 + (\Lambda^- - \zeta(\delta))\Delta T], \tag{A10c}$$

in which the terms $\zeta(\delta)^2\Delta T^2$ and $\Lambda^-\zeta(\delta)\Delta T^2$ were successively neglected given the fact that the terms $\zeta(\delta)^2$ and $\Lambda^-\zeta(\delta)$ are small. Inspection of Eq. (A10c) reveals that the term $\theta(\delta)$ varies linearly with temperature and that the proportionality constant depends on δ. The quantity $\Lambda^- - \zeta(\delta)$ is equivalent to the parameter α_θ in Eq. (15).

*yann.lebouar@onera.fr

[1] J. A. Christodoulides, P. Farber, M. Daniil, H. Okumura, G. C. Hadjipanayis, V. Skumryev, A. Simopoulos, and D. Weller, IEEE Trans. Magn. **37**, 1292 (2001).

[2] D. J. Sellmyer, M. Yu, and R. D. Kirby, Nanostruct. Mater. **12**, 1021 (1999).

[3] S. Okamoto, N. Kikuchi, O. Kitakami, T. Miyazaki, Y. Shimada, and K. Fukamichi, Phys. Rev. B **66**, 024413 (2002).

[4] J. B. Staunton, S. Ostanin, S. S. A. Razee, B. Gyorffy, L. Szunyogh, B. Ginatempo, and E. Bruno, J. Phys.: Condens. Matter **16**, S5623 (2004).

[5] B. W. Roberts, Acta Metall. **2**, 597 (1954).

[6] V. V. Maykov, A. Y. Yermakov, G. V. Ivanova, V. I. Khrabrov, and L. M. Magat, Phys. Met. Metallogr. **67**, 79 (1989).

[7] Y. Endo, K. Oikawa, T. Miyazaki, O. Kitakami, and Y. Shimada, J. Appl. Phys. **94**, 7222 (2003).

[8] S. Mohanan, R. Diebolder, R. Hibst, and U. Herr, J. Appl. Phys. **103**, 07B502 (2008).

[9] Y. K. An, J. W. Liu, and Y. C. Ma, J. Appl. Phys. **103**, 013905 (2008).

[10] T. Seki, T. Shima, K. Takanashi, Y. Takahashi, E. Matsubara, Y. K. Takahashi, and K. Hono, J. Appl. Phys. **96**, 1127 (2004).

[11] Y. K. An, J. W. Liu, Y. C. Ma, and Z. H. Wu, J. Phys. D: Appl. Phys. **41**, 165003 (2008).

[12] T. Hasegawa, W. Pei, T. Wang, Y. Fu, T. Washiya, H. Saito, and S. Ishio, Acta Mater. **56**, 1564 (2008).

[13] B. Yao and K. R. Coffey, J. Appl. Phys. **103**, 07E107 (2008).

[14] M. Chen and D. E. Nikles, Nano Lett. **2**, 211 (2002).

[15] There is a mistake in the equation reported in Refs. 14 and 16: the order parameter should be raised to the power of two, in accordance to Eq. (1).

[16] M. Chen and D. E. Nikles, J. Appl. Phys. **91**, 8477 (2002).

[17] Y. Endo, N. Kikuchi, O. Kitakami, and Y. Shimada, J. Appl. Phys. **89**, 7065 (2001).

[18] C. Leroux, M. C. Cadeville, V. Pierron-Bohnes, G. Inden, and F. Hinz, J. Phys. F: Met. Phys. **18**, 2033 (1988).

[19] T. Mehaddene, E. Kentzinger, B. Hennion, K. Tanaka, H. Numakura, A. Marty, V. Parasote, M. C. Cadeville, M. Zemirli, and V. Pierron-Bohnes, Phys. Rev. B **69**, 024304 (2004).

[20] I. Uszynski, J. Janczak, and R. Kubiak, J. Alloys Compd. **206**, 211 (1994).

[21] R. Tetot, A. Finel, and F. Ducastelle, J. Stat. Phys. **61**, 121 (1990).

[22] Y. Le Bouar, A. Loiseau, and A. Finel, Phys. Rev. B **68**, 224203 (2003).

[23] N. Metropolis, A. W. Rosenbluth, M. N. Rosenbluth, A. H. Teller, and E. Teller, J. Chem. Phys. **21**, 1087 (1953).

[24] M. Fevre, C. Varvenne, Y. Le Bouar, and A. Finel (unpublished).

[25] D. A. Kofke and E. D. Glandt, Mol. Phys. **64**, 1105 (1988).

[26] As opposed to an alloy having a lower critical LROP, which character would be described as having a "weak" first-order character because it would approach the specificity of the continuous transition typical to a second-order transition.

[27] J. Friedel, Philos. Mag. Series 7 **46**, 514 (1955).

[28] M. F. Thorpe and E. J. Garboczi, Phys. Rev. B **42**, 8405 (1990).

[29] E. K. H. Salje, *Phase Transitions in Ferroelastic and Co-elastic Crystals* (Cambridge University Press, Cambridge, England, 1990).

[30] J.-C. Toledano and P. Toledano, *The Landau Theory of Phase*

Transitions (World Scientific, Singapore, 1987).
[31] Y. Wang and A. G. Khachaturyan, Acta Metall. Mater. **43**, 1837 (1995).
[32] Y. Le Bouar, A. Loiseau, and A. G. Khachaturyan, Acta Mater. **46**, 2777 (1998).
[33] E. K. H. Salje, Phys. Rep. **215**, 49 (1992).
[34] B. E. Warren, *X-Ray Diffraction* (Dover, New York, 1990).
[35] C. B. Walker, J. Appl. Phys. **23**, 118 (1952).